Available online at www.sciencedirect.com
SCIENCE DIRECT®
Journal of Solid State Chemistry 178 (2005) 961–969
JOURNAL OF SOLID STATE CHEMISTRY
www.elsevier.com/locate/jssc

Reduction properties of phases in the system $La_{0.5}Sr_{0.5}MO_3$ (M = Fe, Co)

Frank J. Berry[a], José F. Marco[b,*], Xiaolin Ren[a]

[a]*Department of Chemistry, The Open University, Walton Hall, Milton Keynes MK7 6AA, UK*
[b]*Instituto de Química-Física "Rocasolano", Consejo Superior de Investigaciones Científicas, c/ Serrano 119, ES-28006 Madrid, Spain*

Received 5 May 2004; received in revised form 14 September 2004; accepted 4 October 2004

Abstract

Phases formed by the reduction of compounds of the type $La_{0.5}Sr_{0.5}MO_3$ (M = Fe, Co) have been characterized by means of temperature programmed reduction, X-ray powder diffraction, ^{57}Fe Mössbauer spectroscopy and Fe K-, Co K-, Sr K-, and La L_{III}-edge X-ray absorption spectroscopy. The results show that treatment of the material of composition $La_{0.5}Sr_{0.5}FeO_3$ (which contains 50% Fe^{4+} and 50% Fe^{3+}) at 650 °C in a flowing 90% hydrogen/10% nitrogen atmosphere results in the formation of an oxygen-deficient perovskite-related phase containing only trivalent iron. Further heating in the gaseous reducing environment at 1150 °C results in the formation of the Fe^{3+}-containing phase $SrLaFeO_4$, which has a K_2NiF_4-type structure, and metallic iron. The material of composition $La_{0.5}Sr_{0.5}CoO_3$ is more susceptible to reduction than the compound $La_{0.5}Sr_{0.5}FeO_3$ since, after heating at 520 °C in the hydrogen/nitrogen mixture, all the Co^{4+} and Co^{3+} are reduced to metallic cobalt with the concomitant formation of strontium- and lanthanum-oxides.

Keywords: Perovskite-related oxides; Reduction phases; Mössbauer; XAS

1. Introduction

Perovskite-related oxygen-deficient materials of the type $La_{1-y}Sr_yMO_3$ (M = Fe, Co) have been the subject of interest for some time. For example, the cobalt-containing materials have potential applications as electrode materials for high temperature fuel cells, as catalyst in, for example, automobile exhaust catalyst systems, and as gas sensors [1–3]. There is also interest in the unusual magnetic and electronic properties of the materials [4]. Given that some of these applications involve operation under reducing conditions and that the nature of reduced phases in these systems is a matter of sparse attention, we have investigated the nature of materials formed by temperature programmed reduction (TPR) in hydrogen and we report here on their characterization by ^{57}Fe Mössbauer spectroscopy and by X-ray absorption spectroscopy.

2. Experimental

Compounds of the type $La_{0.5}Sr_{0.5}MO_3$ (M = Fe, Co) were prepared by grinding appropriate quantities of lanthanum(III) oxide, strontium(II) carbonate, and either α-iron(III) oxide or cobalt(II) oxide in an agate pestle and mortar and heating in air at 1200 °C (12 h).

X-ray powder diffraction (XRD) patterns were recorded at 298 K with a Siemens D5000 diffractometer using Cu $K\alpha$ radiation. TPR profiles were recorded from ca. 150 mg samples in flowing 10% hydrogen/90% nitrogen (15–20 ml/min) with the temperature being increased by 5 °C/min. Thermal analysis was performed with a Rheometric Scientific STA 1500 system in a 10% hydrogen/90% nitrogen gas mixture flowing at 20 ml/min.

*Corresponding author. Fax: +34 915 642 431.
E-mail address: jfmarco@iqfr.csic.es (J.F. Marco).

0022-4596/$ - see front matter © 2004 Elsevier Inc. All rights reserved.
doi:10.1016/j.jssc.2004.10.003

^{57}Fe Mössbauer spectra were recorded at 298 K with a microprocessor-controlled Mössbauer spectrometer using a ca. 25 mCi ^{57}Co/Rh source. All the spectra were computer fitted and the isomer shift data are reported relative to that of metallic iron at room temperature.

X-ray absorption near edge structure (XANES) and extended X-ray absorption fine structure (EXAFS) measurements were performed at Station 8.1 (Fe K-, Co K-, and La L_{III}-edge) and at Station 9.2 (Sr K-edge) at the Synchrotron Radiation Source at Daresbury Laboratory operating at an energy of 2.0 GeV and an average current of 200 mA. Data were collected at 298 K. The energy scale was calibrated using 6 μm iron and cobalt foils, lanthanum(III) oxide and strontium(II) carbonate. The position of the first inflection point on the iron foil edge was taken at 7112.3 eV, that of the cobalt foil edge at 7708.9 eV, that of lanthanum(III) oxide at 5480.6 eV and that of strontium(II) carbonate at 16,110.2 eV. All the iron-, cobalt-, lanthanum-, and strontium-XANES data are reported here relative to these values. The edge profiles were separated from the EXAFS data and, after subtraction of linear pre-edge background, normalized to the edge step. The position of the absorption edge was obtained from the first most intense maximum of the first derivative of the edge profile. However, since the position of the edge is sometimes defined as the energy at which the normalized absorption is 0.5 (i.e., the absorption at half-height of the edge step) we also quote such values to allow comparison with published data. The EXAFS oscillations were isolated after background subtraction of the raw data using the Daresbury program EXBACK and converted into k space. The data were weighted by k^3, where k is the photoelectron wave vector, to compensate for the diminishing amplitude of EXAFS at high k. The data were fitted using the Daresbury program EXCURV90.

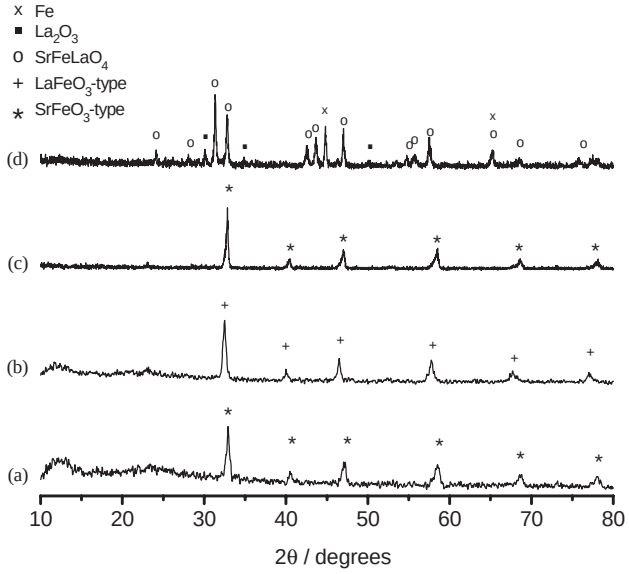

Fig. 1. XRD patterns recorded from (a) $La_{0.5}Sr_{0.5}FeO_3$ and following sequential treatment in (b) 90% hydrogen/10% nitrogen at 650 °C, (c) air at 450 °C, and (d) 90% hydrogen/10% nitrogen at 1150 °C.

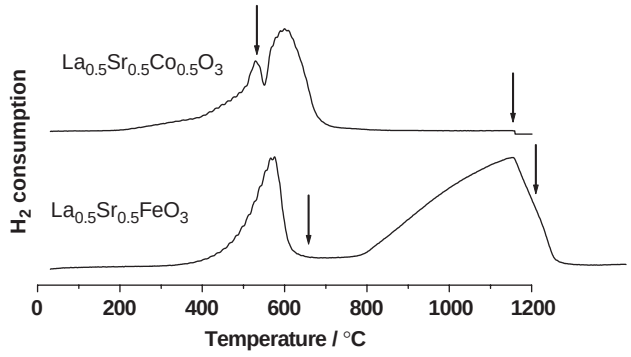

Fig. 2. TPR profiles recorded from $La_{0.5}Sr_{0.5}FeO_3$ and $La_{0.5}Sr_{0.5}CoO_3$.

3. Results and discussion

3.1. $La_{0.5}Sr_{0.5}FeO_3$

The XRD pattern recorded from the compound $La_{0.5}Sr_{0.5}FeO_3$ is shown in Fig. 1a. The pattern is characteristic of the cubic $SrFeO_3$-type structure. The TPR profile recorded from $La_{0.5}Sr_{0.5}FeO_3$ is shown in Fig. 2 and shows an initial narrow peak at ca. 570 °C followed by a broad peak spanning the temperature range ca. 800–1200 °C.

The first reduction peak in the TPR profile recorded from $La_{0.5}Sr_{0.5}FeO_3$ (Fig. 2) was located at a higher temperature than that observed by TPR in $LaFeO_3$ (475 °C) [5]. The XRD pattern (Fig. 1b) recorded from $La_{0.5}Sr_{0.5}FeO_3$ following treatment in the reducing atmosphere at 650 °C, i.e., after the first reduction peak in the TPR profile (Fig. 2), showed all the XRD peaks to shift to lower angle and was more similar to that of the orthorhombic $LaFeO_3$-type phase. No evidence could be found for the presence of strontium oxide. The XRD pattern recorded from the material after reheating in air at 450 °C for 12 h (Fig. 1c) showed the product to return to the cubic $SrFeO_3$-type structure. The XRD pattern recorded from the material following treatment by TPR at 1150 °C (Fig. 1d) showed the formation of $SrFeLaO_4$, which adopts the K_2NiF_4-type structure [6], La_2O_3, and metallic iron.

The ^{57}Fe Mössbauer spectra recorded at 298 K are shown in Fig. 3. The spectrum recorded from the pure material (Fig. 3a) showed a broad absorption line which was best fitted to two singlet components. The results of the fit are collected in Table 1. The isomer shift of the

singlet appearing at lower velocity is characteristic of Fe^{4+} in octahedral oxygen coordination [7] whilst the parameters of the other singlet correspond to Fe^{3+}. A comparison of the spectral areas of both components (Table 1) indicates that the material contains equal amounts of Fe^{4+} and Fe^{3+}.

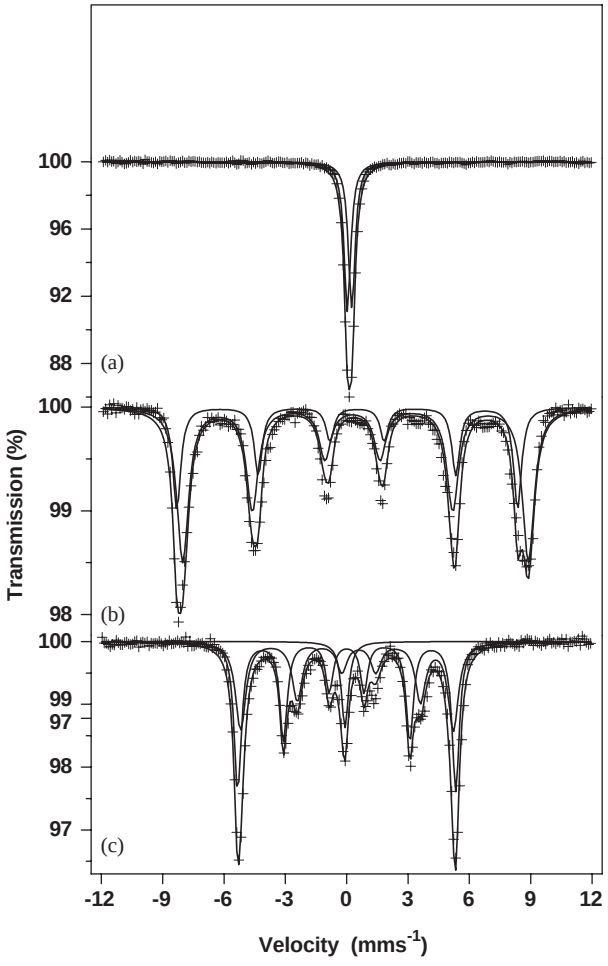

Fig. 3. (a) ^{57}Fe Mössbauer spectra recorded at 298 K from (a) $La_{0.5}Sr_{0.5}FeO_3$ and following treatment in 90% hydrogen/10% nitrogen at (b) 650 °C and (c) 1150 °C.

The spectrum recorded following treatment in flowing hydrogen and nitrogen (Fig. 3b) at ca. 650 °C (i.e., after the first peak in the TPR profile, Fig. 2) showed the superposition of two magnetically split sextet components both characteristic of Fe^{3+} (Table 1) and demonstrating that low temperature treatment induces reduction of Fe^{4+}–Fe^{3+}. The shift in the XRD peak positions to lower angle (Fig. 2b) indicated an increase in unit cell parameters from $a = 5.490(1)$ Å, $c = 13.38(1)$ Å for $La_{0.5}Sr_{0.5}FeO_3$ to $a = 5.533(1)$ Å, $c = 13.50(1)$ Å for the partially reduced sample consistent with the presence of an increasing amount of Fe^{3+} with larger ionic radius. The results of thermal analysis of $La_{0.5}Sr_{0.5}FeO_3$ in 10% hydrogen/90% nitrogen are shown in Fig. 4. A weight decrease of ca. 2% corresponding to a loss of lattice oxygen and the formation of a material of a composition $La_{0.5}Sr_{0.5}FeO_{2.72}$ was observed from the thermogravimetric analysis (TGA) curve at ca. 600 °C. This agrees well with the formation of a compound of formula $La_{0.5}Sr_{0.5}FeO_{2.75}$ which can be calculated on the assumption that all the Fe^{4+} in $La_{0.5}Sr_{0.5}FeO_3$ is reduced to Fe^{3+}. The identification of two sextet patterns is indicative of two Fe^{3+} sites. The sextet with smaller chemical isomer shift ($\delta = 0.27$ mm s^{-1}) is characteristic of Fe^{3+} in coordination lower than octahedral, as has been observed previously in other oxygen-deficient perovskite-related materials [8], whilst the other sextet is characteristic of Fe^{3+} in octahedral sites. It is interesting to note that while the pure material is paramagnetic at room temperature, the material obtained after treatment in the flowing hydrogen and nitrogen at 650 °C is magnetically ordered at 298 K. This can be associated with the different strengths of magnetic interactions operating in these compounds. It is known [9] that the Fe^{3+}–Fe^{3+} interaction is stronger than Fe^{4+}–Fe^{4+} and Fe^{4+}–Fe^{3+} interactions.

Table 1
^{57}Fe Mössbauer parameters recorded from $La_{0.5}Sr_{0.5}FeO_3$ following treatment in 90% hydrogen/10% nitrogen

	Assignment	$\delta \pm 0.01$ (mm s^{-1})	Δ [a] or 2ε [b] ± 0.02 (mm s^{-1})	$\Gamma \pm 0.02$ (mm s^{-1})	$H \pm 0.5$ (T)	Spectral area $\pm 3\%$
$La_{0.5}Sr_{0.5}FeO_3$	Fe^{4+}	0.03	0	0.39	0	50
	Fe^{3+}	0.25	0	0.39	0	50
Following treatment in 90%	Fe^{3+}	0.27	–0.40	0.61	52.1	47
hydrogen/10% nitrogen at 650 °C	Fe^{3+}	0.37	0.19	0.61	52.9	53
1150 °C	Fe^{3+}	0.31	0.58	0.60	32.4	42
	Fe^{0}	0.00	0	0.43	33.2	51
	Fe^{0}	−0.08	0	0.42	0	7

[a]Quadrupole split absorption.
[b]Magnetically split absorption.

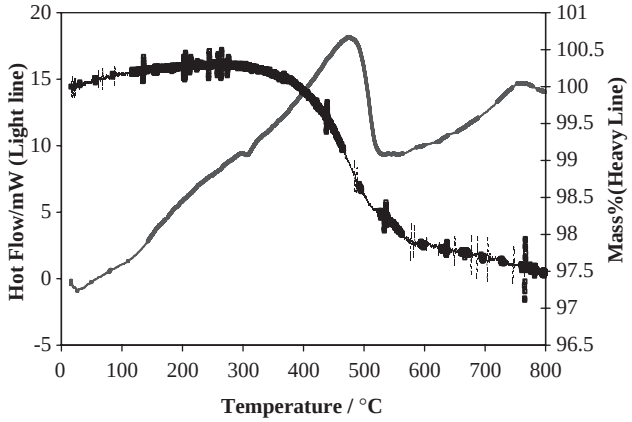

Fig. 4. TGA (heavy line) and DSC (light line) curves recorded from $La_{0.5}Sr_{0.5}FeO_3$ in flowing 10% hydrogen/90% nitrogen.

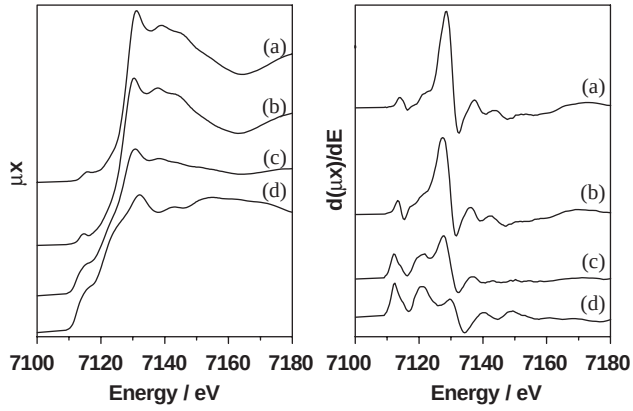

Fig. 5. (Left) Iron K-edge XANES recorded from (a) $La_{0.5}Sr_{0.5}FeO_3$ and following treatment in 90% hydrogen/10% nitrogen at (b) 650 °C and (c) 1150 °C. (d) Iron K-edge XANES recorded from metallic iron. (Right) Corresponding first derivatives of the data.

Therefore, the presence of only Fe^{3+} ions in the material heated at 650 °C in hydrogen and nitrogen results in stronger superexchange interactions than in the original material and, therefore, in magnetic order at room temperature and in the existence of a hyperfine magnetic field.

The spectrum recorded from the material heated at ca. 1250 °C, that is, after the second peak in the TPR profile showed the superposition of two sextets and a singlet (Fig. 3c). One of the sextets, characteristic of Fe^{3+} (δ = ca. 0.31 mm s^{-1}), demonstrated a small hyperfine magnetic field (H = ca. 32.4 T). The parameters are similar to those reported [6] for $LaSrFeO_4$ which adopts the K_2NiF_4-type structure. The other sextet (H = ca. 33.2 T) and the singlet (δ = ca. 0.08 mm s^{-1}) are characteristic of large- and small-particle metallic α-iron, respectively [5]. Hence, treatment of $La_{0.5}Sr_{0.5}FeO_3$ at elevated temperature in a mixture of flowing hydrogen and nitrogen induces both structural rearrangement of the perovskite-related lattice to the K_2NiF_4-type structure and reduction to metallic iron. It is worth noting that, even after treatment at the high temperature in the reducing atmosphere, a noticeable amount of iron remains in the trivalent state.

The Fe K-edge XANES (and their first derivative) recorded from pure $La_{0.5}Sr_{0.5}FeO_3$ and the materials obtained after treatment at 650 and 1150 °C are shown in Fig. 5 together with the Fe K-edge XANES of metallic iron used as a reference. The position of the absorption edge in the Fe K-edge XANES of $La_{0.5}Sr_{0.5}FeO_3$ appears at ca. 7128.5 eV (Table 2). This is ca. 1.9 eV higher than the position of the Fe K-edge absorption edge of $LaFeO_3$ that only contains trivalent iron. It has been recently reported [10] that the energy difference between the point at half absorption in the

Table 2
X-ray absorption edge positions recorded from the X-ray absorption near edge structure

	Edge position[a] (eV) ± 0.3				Edge position[b] (eV) ± 0.3			
	Fe	Co	La	Sr	Fe	Co	La	Sr
Fe (metal foil)	7119.7	—	—	—	7112.3	—	—	—
Co (metal foil)	—	7716.0	—	—	—	7709.0	—	—
$LaFeO_3$	7125.5	—	5482.3	—	7126.6	—	5484.3	—
$LaCoO_3$	—	7720.6	—	—	—	7723.6	—	—
La_2O_3	—	—	5480.6	—	—	—	5484.3	—
$SrCO_3$								16,110.2
$La_{0.5}Sr_{0.5}FeO_3$	7126.5	—	5480.2	16,102.5	7128.5	—	5483.5	16,110.2
(TPR treated) 650 °C	7124.9	—	5480.2	16,104.3	7127.4	—	5483.4	16,110.2
(TPR treated) 1250 °C	7121.9	—	5480.2	16,103.8	7112.3	—	5483.2	16,110.2
$La_{0.5}Sr_{0.5}CoO_3$	—	7721.8	5480.5	16,105.1	—	7724.2	5483.9	16,110.0
(TPR treated) 520 °C	—	7716.6	5480.8	16,105.0	—	7709.0	5483.9	16,110.2
(TPR treated) 1150 °C	—	7716.2	5481.0	16,104.9	—	7709.0	5484.2	16,110.2

[a]Corresponds to the absorption at half-height of the edge step.
[b]Corresponds to the first most intense maximum in the derivative of the XANES.

edge step of $SrFeO_{3-\delta}$ (a material in which iron is mainly present as Fe^{4+}) and the first inflexion point in the Fe K-edge XANES of metallic iron is ca. 14 eV. Inspection of Table 2 shows a similar energy difference between $La_{0.5}Sr_{0.5}FeO_3$ and metallic iron. The results are consistent with the presence of Fe^{4+} in this material as indicated by Mössbauer spectroscopy. The position of the Fe K-absorption edge recorded from the material following treatment at 650 °C shifted to 7127.4 eV, a value that is closer to that of $LaFeO_3$. It is also interesting to note that the $1s \rightarrow 3d$ pre-edge feature at 7115.9 eV in the Fe K-edge XANES of pure $La_{0.5}Sr_{0.5}FeO_3$ shifts to 7114.6 eV in the Fe K-edge XANES of the material treated at 650 °C. A shift of ca. 1.5 eV is also observed at the edge crest (Fig. 5). All these changes are indicative of the reduction of Fe^{4+}–Fe^{3+} as shown by Mössbauer spectroscopy. Furthermore, inspection of Fig. 5 suggests that the pre-edge feature in the Fe K-edge XANES of $La_{0.5}Sr_{0.5}FeO_3$ (characteristic of distorted octahedral geometry) increases in intensity in the Fe K-edge XANES of the material treated under the reducing atmosphere at 650 °C. This is compatible with the existence of a fraction of Fe^{3+} in coordination lower than octahedral [11] as also shown by Mössbauer spectroscopy. Finally, the first most intense maximum in the derivative of the Fe K-edge XANES of the material treated at 1150 °C appears at 7112.3 eV, a value which coincides with the position of the Fe K-edge of metallic iron. Inspection of Fig. 5 also shows that the Fe K-edge XANES of this material contains some features compatible with the presence of Fe^{3+} (e.g., peak in the first derivative at 7127.4 eV) which corresponds with the presence of the Fe^{3+}-containing phase $SrLaFeO_4$ as identified also by both XRD and ^{57}Fe Mössbauer spectroscopy. Summarizing, the movement to lower energy of the X-ray absorption Fe K-edge XANES (clearly observed in Fig. 5 and Table 2 if the criterion of defining the position of the edge as the energy at half-height of the edge step is taken) with increasing treatment in the hydrogen/nitrogen gas mixture is consistent with reduction of iron. In contrast to the variation of the Fe K-edge X-ray absorption edge positions, the La L_{III}-edge- and Sr K-edge-X-ray absorption edge positions did not change significantly with treatment in the flowing mixture of hydrogen and nitrogen being characteristic of La^{3+} and Sr^{2+}, respectively (Table 2).

The Fe K-edge EXAFS is shown in Fig. 6, top. The fitting of the data recorded from the reduced materials was complicated by the multiphasic nature of the products; hence, Table 3 contains only the best fit parameters in the region 0–4 Å. The first peak corresponding to six oxygen atoms in the Fourier transform of the data recorded from $La_{0.5}Sr_{0.5}FeO_3$ (Fig. 6a, bottom) was located at ca. 1.92 Å which is shorter than the distances (1.98–2.00 Å) for the six oxygen atoms

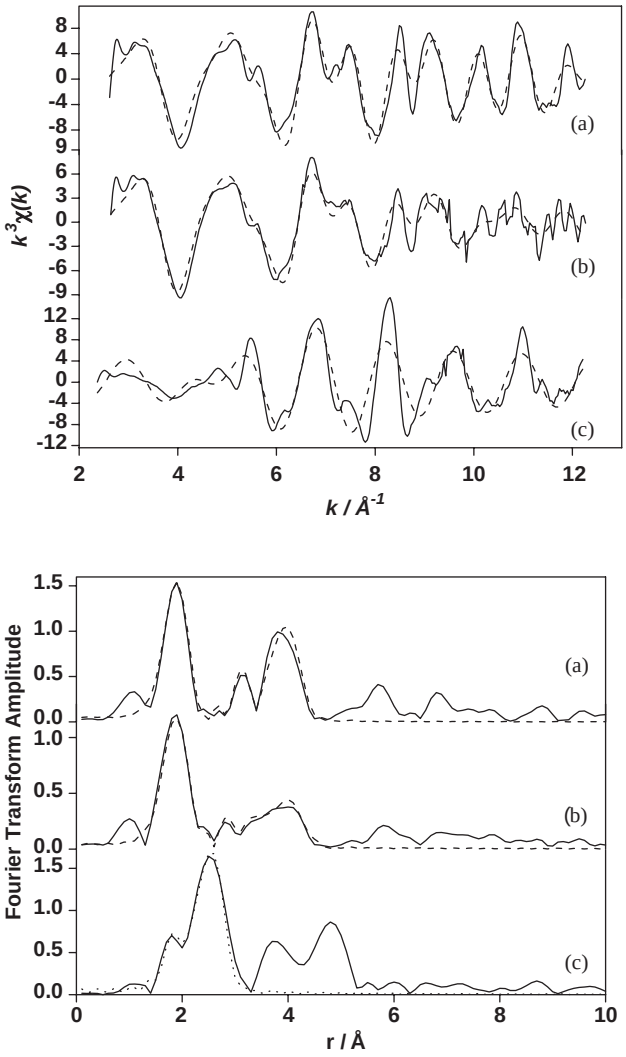

Fig. 6. (Top) Fe K-edge EXAFS recorded from (a) $La_{0.5}Sr_{0.5}FeO_3$ and following treatment in 90% hydrogen/10% nitrogen at (b) 650 °C and (c) 1150 °C. (Bottom) The corresponding Fourier transforms of the EXAFS. (The experimental data are indicated by the solid line and the fits to the data are indicated by the broken line.)

which coordinate iron in $LaFeO_3$ [5,12]. This is consistent with the presence of Fe^{4+} in $La_{0.5}Sr_{0.5}FeO_3$ as shown by ^{57}Fe Mössbauer spectroscopy. A better fit was obtained by refining the first shell oxygen coordination to three oxygen atoms at 1.87 Å, a distance which is characteristic of Fe^{4+} [13], and three at 1.98 Å which reflects the equal amount of Fe^{4+} and Fe^{3+} in this material.

Following treatment in hydrogen and nitrogen at 650 °C the Fe K-edge EXAFS showed the first shell of six oxygen atoms to be located at ca. 1.94 Å and to be best separated into three oxygen atoms at 1.89 Å and three at 2.00 Å (Table 3). The results suggest that, in the material resulting from treatment in hydrogen and nitrogen at 650 °C, half of the Fe^{3+} are in lower coordination than octahedral. In this respect, we would

Table 3
Best fit parameters to the EXAFS data recorded from $La_{0.5}Sr_{0.5}FeO_3$

	$La_{0.5}Sr_{0.5}FeO_3$			$La_{0.5}Sr_{0.5}FeO_3$ treated at 650 °C			$La_{0.5}Sr_{0.5}FeO_3$ treated at 1250 °C		
	Coordination number and [atom type]	d (Å) ($\pm$0.02)	$2\sigma^2$ (Å^2)	Coordination number and [atom type]	d (Å) ($\pm$0.02)	$2\sigma^2$ (Å^2)	Coordination number and [atom type]	d (Å) ($\pm$0.02)	$2\sigma^2$ (Å^2)
Fe K-edge	3 [O]	1.87	0.006	3 [O]	1.89	0.011	4 [O]	1.96	0.019
	3 [O]	1.98	0.004	3 [O]	2.00	0.015	2 [O]	2.20	0.012
	8 [La]	3.21	0.033	8 [La]	3.19	0.034	4.5 [Fe]	2.48	0.013
	6 [Fe]	3.94	0.009	6 [Fe]	3.95	0.023			
La L_{III}-edge	3 [O]	2.59	0.007	3 [O]	2.53	0.015	1 [O]	2.44	0.003
	6 [O]	2.81	0.031	6 [O]	2.74	0.039	4 [O]	2.63	0.001
	3 [O]	3.49	0.004	3 [O]	3.47	0.049	4 [O]	2.85	0.002
Sr K-edge	3 [O]	2.56	0.011	3 [O]	2.54	0.020	1 [O]	2.39	0.001
	6 [O]	2.75	0.024	6 [O]	2.76	0.056	4 [O]	2.59	0.004
	3 [O]	3.32	0.001	3 [O]	3.30	0.001	4 [O]	2.79	0.010

mention that a tentative structure has been proposed for the perovskite-related oxide of composition $SrFeO_{2.75}$ [8] in which every other oxygen atom is lost from certain strings such that half of the iron ions remains octahedrally coordinated and half become five coordinated. Also, in the reduced phase of formula $La_{1-2x}Ca_{2x}FeO_{3-x}$ which contains only Fe^{3+}, the existence of tetrahedral sites has been confirmed for x values as small as 0.10 [8]. In the absence of more structural data, we cannot decide whether the sextet with the lower isomer shift arises from five coordinated or tetrahedrally coordinated Fe^{3+}. However, if this material formed by partial reduction at 650 °C contained equal quantities of octahedrally and tetrahedrally coordinated Fe^{3+} then an oxygen content of 2.5, as in the ordered brownmillerite structure in which each tetrahedrally coordinated iron is surrounded by two oxygen vacancies, would be required which is not the case.

The first shell coordination of iron in the Fe K-edge EXAFS recorded from $La_{0.5}Sr_{0.5}FeO_3$ following treatment in flowing hydrogen and nitrogen at 1150 °C was fitted according to the evidence from XRD and Mössbauer spectroscopy for reduction to $LaSrFeO_4$ and metallic iron. Hence, the coordination of iron by four oxygen atoms at 1.96 Å and two at 2.20 Å agrees well with the neutron diffraction data recorded form $LaSrFeO_4$ [6] whilst the iron atoms at ca. 2.48 Å represent the metallic iron (Fig. 6c, bottom and Table 3).

The La L_{III}-edge and Sr K-edge EXAFS (Table 3) recorded from $La_{0.5}Sr_{0.5}FeO_3$ showed lanthanum and strontium to be coordinated by 12 oxygen atoms as would be expected given the evidence from XRD that the material adopts the cubic $SrFeO_3$-type structure. The material treated in hydrogen at ca. 650 °C showed little change in the first shell oxygen coordination of lanthanum and strontium (Table 3). Treatment in the 90% hydrogen/10% nitrogen gas mixture at 1150 °C induced a change in the first shell coordination of lanthanum and strontium to nine oxygen atoms (Table 3). This is in good agreement with the XRD pattern (Fig. 1d) that showed the formation of $LaSrFeO_4$, which contains lanthanum and strontium in nine-fold oxygen coordination [6].

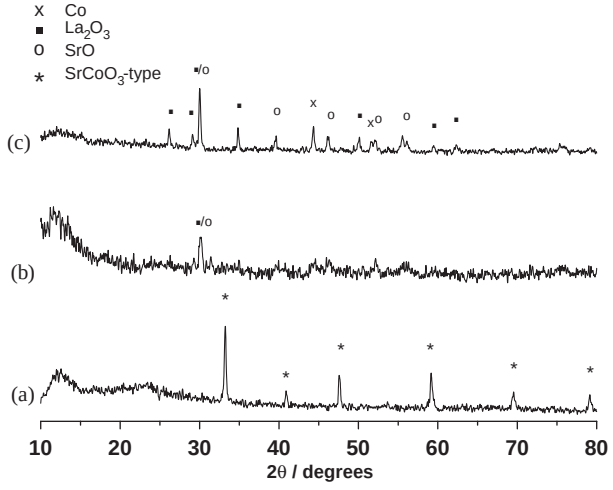

Fig. 7. XRD patterns recorded from (a) $La_{0.5}Sr_{0.5}CoO_3$ and following sequential treatment in 90% hydrogen/10% nitrogen at (b) 520 °C and (c) 1150 °C.

3.2. $La_{0.5}Sr_{0.5}CoO_3$

The XRD pattern recorded from the compound $La_{0.5}Sr_{0.5}CoO_3$ is shown in Fig. 7a. The pattern is characteristic of the $SrCoO_3$-type structure. The TPR profile recorded from $La_{0.5}Sr_{0.5}CoO_3$ (Fig. 2) showed the second peak to move to much lower temperature as

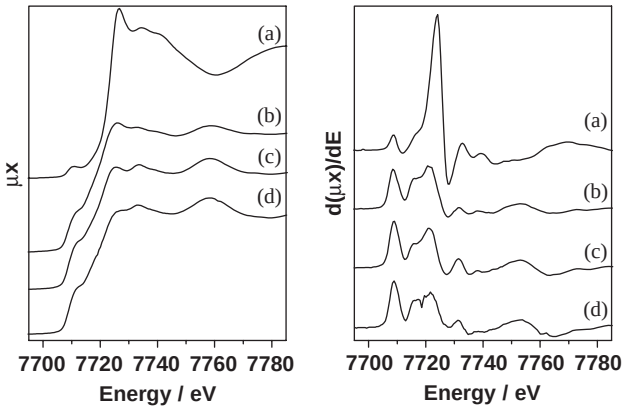

Fig. 8. (Left) Co K-edge XANES recorded from (a) $La_{0.5}Sr_{0.5}CoO_3$ and following treatment in flowing 90% hydrogen/10% nitrogen at (b) 520 °C and (c) 1150 °C. (d) Co K-edge XANES recorded from metallic cobalt. (Right) Corresponding first derivatives of the data.

compared to that recorded from $La_{0.5}Sr_{0.5}FeO_3$. The XRD pattern recorded from the material treated at 520 °C (Fig. 7b), i.e., after the first reduction peak in the TPR profile (Fig. 2), showed the material to be poorly crystalline but to contain broad peaks which may be associated with the most intense peaks of strontium- and lanthanum-oxides. After TPR treatment at 1150 °C, the material had decomposed to strontium- and lanthanum-oxides and metallic cobalt (Fig. 7c).

The X-ray absorption edge position at 7724.2 eV of the Co K-edge XANES recorded from $La_{0.5}Sr_{0.5}CoO_3$ (Fig. 8a, Table 2) is ca. 0.6 eV larger than the edge position of the Co K-edge XANES recorded from $LaCoO_3$ [5], a material which contains only trivalent cobalt. The energy at half-height of the edge step (Table 2) correlates well with recently published XANES data for $La_{0.5}Sr_{0.5}CoO_3$ [14,15] and reflects the presence in this compound of Co^{4+} and Co^{3+}. The Co K-edge XANES recorded from the material following treatment in flowing hydrogen and nitrogen at 520 °C was almost identical to that recorded from metallic cobalt (Fig. 8b and 7d). The result demonstrates that, under these mild conditions, the formation of metallic cobalt is readily achieved (see also Table 2). The Co K-edge XANES recorded from the material heated in the reducing atmosphere at the higher temperature of 1150 °C also showed the presence of metallic cobalt (Fig. 8c).

The Co K-edge EXAFS (Fig. 9, Table 4) endorsed the XANES data. The EXAFS data recorded from $La_{0.5}Sr_{0.5}CoO_3$ were initially fitted to six oxygen atoms (Fig. 9a, bottom) at 1.90 Å, a value close to that reported previously for cobalt–oxygen distances in $La_{0.5}Sr_{0.5}CoO_3$ [14,15]. A better fit was obtained by adopting the approach used to fit the data from $La_{0.5}Sr_{0.5}FeO_3$, and involving fitting the data to a model in which the first oxygen shell was split (Table 4) to a set

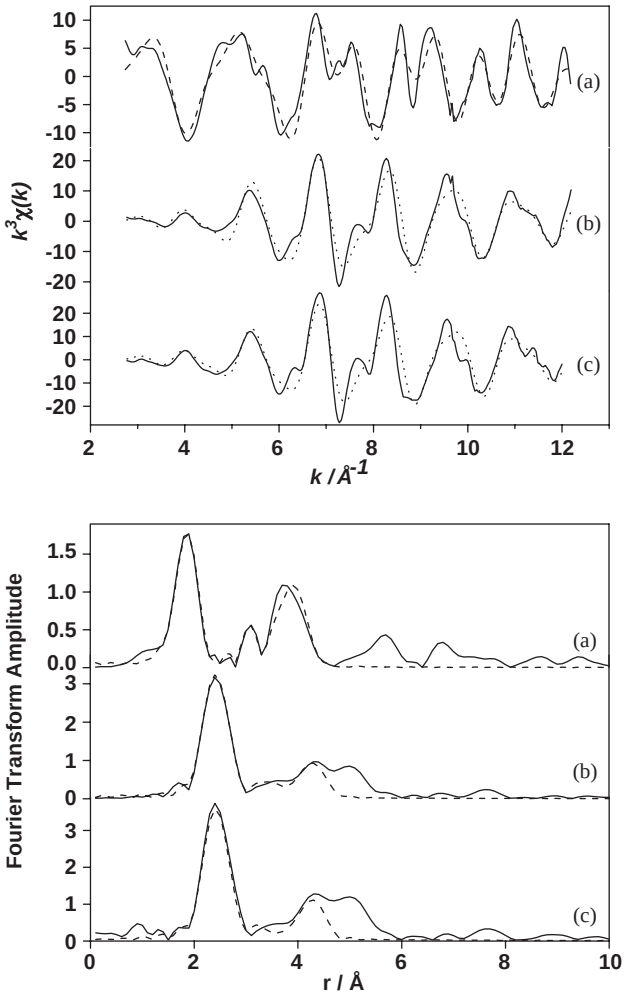

Fig. 9. (Top) Co K-edge EXAFS recorded from (a) $La_{0.5}Sr_{0.5}CoO_3$ and following treatment in flowing 90% hydrogen/10% nitrogen at (b) 520 °C and (c) 1150 °C. (Bottom) The corresponding Fourier transforms of the above EXAFS. (The experimental data are indicated by the solid line and the fits to the data are indicated by the broken line.)

of three oxygen atoms at a distance of 1.85 Å (corresponding to the presence of Co^{4+} in this material) and three oxygen atoms at a distance of 1.96 Å (accounting for Co^{3+}). In contrast, the EXAFS recorded from the reduced phases showed only the coordination of cobalt by cobalt (Fig. 9b and c, bottom and Table 4).

The X-ray absorption edge position of the La_{III}- and Sr K-edges obtained from the XANES data (Table 2) did not change significantly with treatment in the reducing environment. The La L_{III}-edge EXAFS recorded from $La_{0.5}Sr_{0.5}CoO_3$ (Fig. 10a, Table 4) showed the lanthanum to be coordinated to 12 oxygen atoms in the perovskite-related structure [16]. Treatment at 520 and 1150 °C in flowing hydrogen and nitrogen gave seven-fold oxygen coordination characteristic of La_2O_3 [17] (Fig. 10b and c, Table 4). The Sr K-edge EXAFS recorded from $La_{0.5}Sr_{0.5}CoO_3$ (Fig. 11a, Table 4)

Table 4
Best fit parameters to the EXAFS data recorded from $La_{0.5}Sr_{0.5}CoO_3$

	$La_{0.5}Sr_{0.5}CoO_3$			$La_{0.5}Sr_{0.5}CoO_3$ treated at 520 °C			$La_{0.5}Sr_{0.5}CoO_3$ treated at 1150 °C		
	Coordination number and [atom type]	d (Å) ($\pm$0.02)	$2\sigma^2$ (Å^2)	Coordination number and [atom type]	d (Å) ($\pm$0.02)	$2\sigma^2$ (Å^2)	Coordination number and [atom type]	d (Å) ($\pm$0.02)	$2\sigma^2$ (Å^2)
Co K-edge	3 [O]	1.85	0.005	8 [Co]	2.48	0.014	8 [Co]	2.48	0.012
	3 [O]	1.96	0.004	6 [Co]	3.49	0.028	6 [Co]	2.45	0.035
	8 [La]	3.17	0.031	12 [Co]	4.31	0.018	12 [Co]	4.30	0.015
	6 [Co]	3.89	0.009						
La L_{III}-edge	3 [O]	2.55	0.002	4 [O]	2.52	0.004	4 [O]	2.52	0.003
	6 [O]	2.74	0.020	3 [O]	2.70	0.006	3 [O]	2.67	0.007
	3 [O]	3.41	0.008						
Sr K-edge	3 [O]	2.58	0.003	6 [O]	2.55	0.024	6 [O]	2.57	0.021
	6 [O]	2.77	0.014	4 [Sr]	3.54	0.041	12 [Sr]	3.61	0.045
	3 [O]	3.28	0.003						

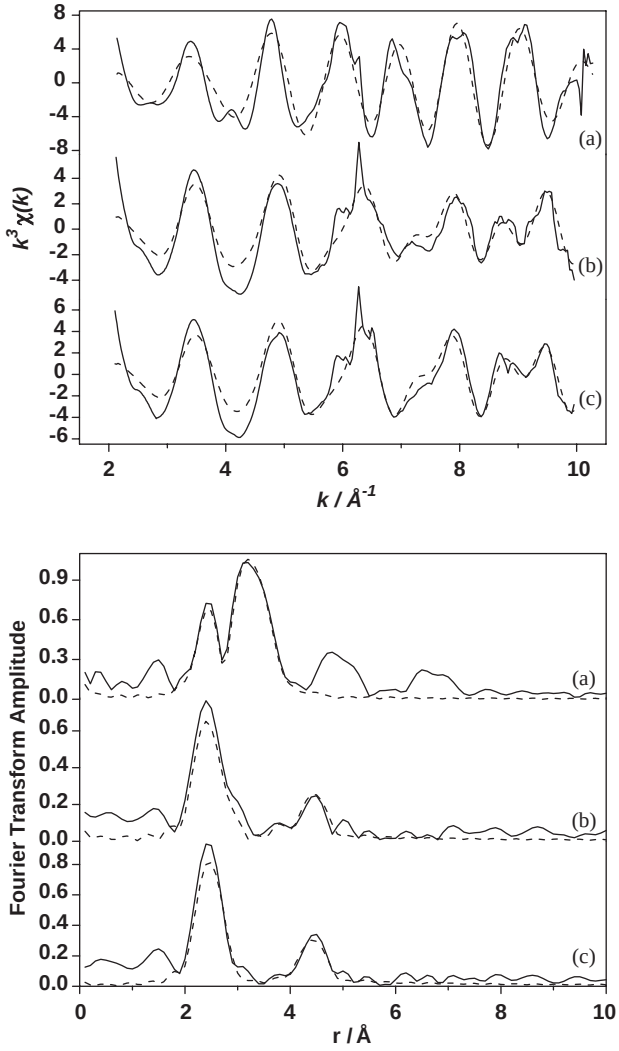

Fig. 10. (Top) La L_{III}-edge EXAFS recorded from (a) $La_{0.5}Sr_{0.5}CoO_3$ and following treatment in flowing 90% hydrogen/10% nitrogen at (b) 520 °C and (c) 1150 °C. (Bottom) The corresponding Fourier transforms of the above EXAFS. (The experimental data are indicated by the solid line and the fits to the data are indicated by the broken line.)

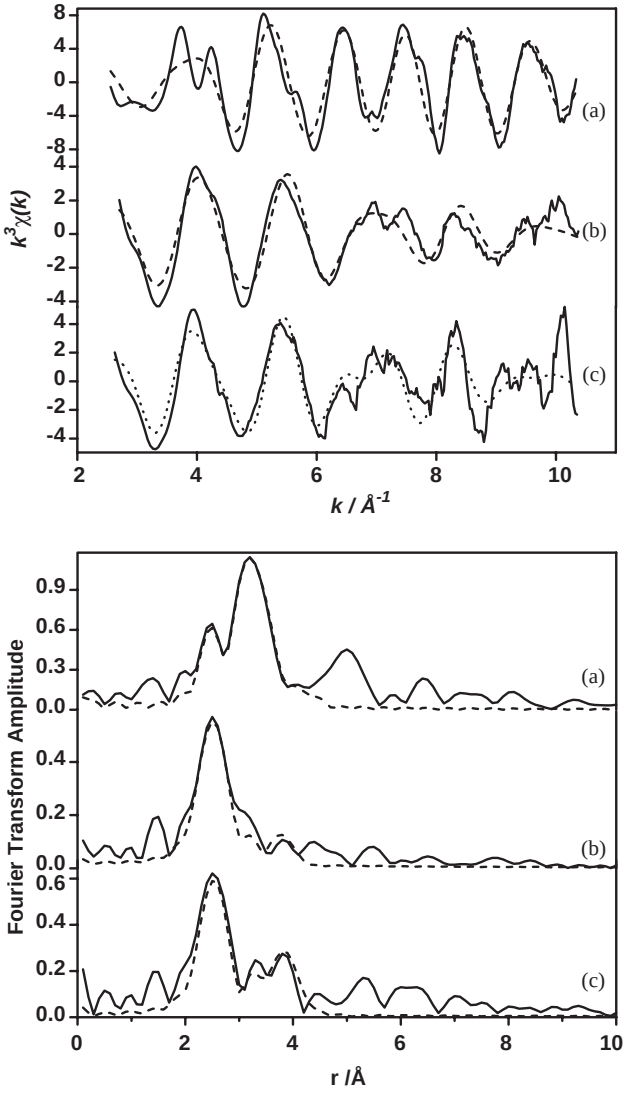

Fig. 11. (Top) Sr K-edge EXAFS recorded from (a) $La_{0.5}Sr_{0.5}CoO_3$ and following treatment in flowing 90% hydrogen/10% nitrogen at (b) 520 °C and (c) 1150 °C. (Bottom) The corresponding Fourier transforms of the above EXAFS. (The experimental data are indicated by the solid line and the fits to the data are indicated by the broken line.)

showed the strontium to be coordinated to 12 oxygen atoms in the perovskite-related structure. The data recorded following treatment in hydrogen and nitrogen at 520 and 1150 °C (Fig. 11b and c, Table 3) showed the strontium atom to be coordinated to six oxygen atoms at a distance of ca. 2.55–2.57 Å characteristic of the rock salt-related strontium oxide structure.

4. Conclusion

The results show that treatment of the material of composition $La_{0.5}Sr_{0.5}FeO_3$ (which contains 50% Fe^{4+} and 50% Fe^{3+}) at 600 °C in a flowing 90% hydrogen/10% nitrogen atmosphere results in the formation of an oxygen-deficient perovskite-related phase containing only trivalent iron. Further heating at 1150 °C results in the formation of the Fe^{3+}-containing phase SrLa FeO_4, which has a K_2NiF_4-type structure, and metallic iron. The material of composition $La_{0.5}Sr_{0.5}CoO_3$ is more susceptible to reduction than the compound $La_{0.5}Sr_{0.5}FeO_3$ since after heating at 520 °C in the reducing hydrogen/nitrogen atmosphere all the Co^{4+} and Co^{3+} present in the original material is reduced to metallic cobalt with the concomitant formation of strontium- and lanthanum-oxides. The results show that in perovskite-related phases of the type $La_{0.5}Sr_{0.5}$ MO_3 (M = Fe, Co) the cobalt-containing variant is more amenable to reduction in reducing gaseous environments that its iron-containing counterpart.

References

[1] Y. Nishihata, J. Mizuki, T. Akao, H. Tanaka, M. Uenishi, M. Kimura, T. Okamoto, H. Hamada, Nature 418 (2002) 164.
[2] T. Nakamoro, M. Misona, Y. Yoneda, J. Catal. 83 (1983) 151.
[3] J. Ohno, S. Nagata, H. Sato, Solid State Ionics 3–4 (1981) 439.
[4] G. Briceno, X.-D. Xiang, H. Chang, X. Sun, P.G. Schulz, Science 270 (1995) 273.
[5] F.J. Berry, X. Ren, J. Gancedo, J.F. Marco, J. Solid State Chem. 17 (2004) 2101.
[6] J.L. Soubeyroux, P. Courbin, L. Fournès, D. Fruchart, G. Le Flem, J. Solid State Chem. 31 (1980) 313–320.
[7] L. Fournès, A. Wattiaux, A. Demourgues, P. Bezdicka, J.C. Grenier, M. Pouchard, J. Etourneau, J. Phys. IV, Colloque C1 7 (1997) C1-353.
[8] T.C. Gibb, J. Chem. Soc. Dalton Trans. (1985) 1455.
[9] J.B. Yang, W.B. Yelon, W.J. James, Z. Chu, M. Kornecki, Y.X. Xie, X.D. Zhou, H.U. Anderson, A.G. Joshi, S.K. Malik, Phys. Rev. B 66 (2002) 184415.
[10] G.M. Veith, I.D. Fawcett, M. Greenblatt, M. Croft, I. Nowik, Int. J. Inorg. Mater. 2 (2000) 513.
[11] G.A. Waychunas, M.J. Apted, G.E. Brown, J. Phys. Chem. Miner. 10 (1983) 1.
[12] H. Falcon, A.E. Goeta, G. Punte, R.E. Carbonio, J. Solid State Chem. 133 (1997) 379.
[13] M. Holzapfel, O. Proux, P. Strobel, C. Darie, M. Borowski, M. Morcrette, J. Mater. Chem. 14 (2004) 102.
[14] A.C. Masset, O. Toulemonde, D. Pelloquin, E. Suard, A. Maignan, F. Studer, M. Hervieu, C. Michel, Int. J. Inorg. Mater. 2 (2000) 687.
[15] J.E. Sunstrom IV, K.V. Ramanujachary, M. Greenblatt, J. Solid State Chem. 139 (1998) 388.
[16] P. Porta, S. de Rossi, M. Faticanti, G. Minelli, I. Pettiti, L. Lisi, M. Turco, J. Solid State Chem. 146 (1999) 291.
[17] F. Ali, A.V. Chadwick, M.E. Smith, J. Mater. Chem. 7 (1997) 285.